PERSPECTIVE

Check for updates

The sweetest polymer nanoparticles: opportunities ahead for glycogen in nanomedicine

Quinn A. Besford (ID)

Most cells take simple sugar (α-D-glucose) and assemble it into highly dense polysaccharide nanoparticles called glycogen. This is achieved through the action of multiple coupled-enzymatic reactions, yielding the cellular store of polymerised glucose to be degraded in times of metabolic need. These nanoparticles can be readily isolated from various animal tissues and plants, and are commercially available on a large scale. Importantly, glycogen is highly water soluble, non-toxic, low-fouling, and biodegradable, making it an attractive nanoparticle for use in nanomedicine, for both diagnosing and treating disease. This concept has been pursued actively recently, with exciting results on a variety of fronts, especially for targeting specific tissues and delivering nucleic acid and peptide cargo. In this perspective, the role of glycogen in nanomedicine going forward is discussed, with opportunities highlighted of where these sugary nanoparticles fit into the problem of treating disease.

Introduction

Most cells, eukaryotic and prokaryotic,[1] store glucose as dense and randomly hyperbranched[2] polysaccharide nanoparticles called glycogen. Glycogen nanoparticles are composed of linear chains of α-1,4-D-glucose, with branching *via* α-1,6-D-glucose linkages (Fig. 1), which are assembled through multiple enzymatic reactions that correspond with the metabolic need/excess of the cell. These nanoparticles, initially reported back in 1857 by Claude Bernard who isolated glycogen from liver tissue,[3] are directly implicated in metabolism and in metabolic diseases. This has meant that research on glycogen over the last many decades has largely been focused on its role in disease, particularly on the numerous glycogen storage diseases[4] and diabetes.[2] Yet despite its relevance and importance in these diseases, glycogen is also a biomaterial nanoparticle that can be nano-engineered for performing therapeutic functions within the context of nanomedicine. A concept where the nanoparticle can be taken from biology and reinserted with a therapeutic purpose. This is attractive for numerous reasons, including glycogen's high-water solubility, ideal size (<100 nm),[5] biocompatibility and biodegradability, but also due to the circularity; glycogen can be readily isolated from renewable sources, commercially available on a large scale, and the degradation products are mainly glucose and a small amount of protein.

Whilst the use of glycogen as an advanced material has been reviewed recently,[6] there has been a flurry of recent exciting
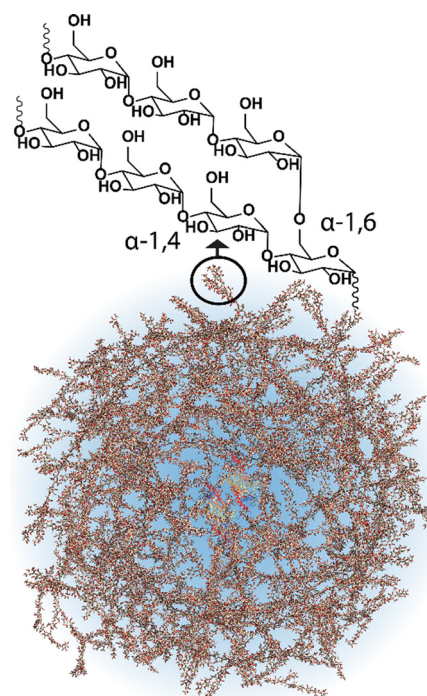

Fig. 1 Schematic of a glycogen nanoparticle with the internal chain structure shown. Reprinted in part with permission from ref. 6. Copyright 2020 John Wiley and Sons.

Leibniz-Institut für Polymerforschung Dresden e.V., Hohe Str. 6, Dresden 01069, Germany. E-mail: besford@ipfdd.de

works since that show this nanoparticle can do much in nanomedicine, at times better than or similar to synthetic materials, and other biomaterials, particularly for in-blood and in-tissue interactions. It is highly desirable to transition to minimally synthetic, renewable, biocompatible materials in the pharmaceutical sciences, where polysaccharide biomaterials are key candidates.[7] Glycogen is a polysaccharide that ticks many required boxes in this pursuit. In this perspective, the opportunities for biomaterial glycogen nanoparticles in nanomedicine is discussed in detail.

Glycogen metabolism

The synthesis of glycogen is the result of multiple coupled enzymatic reactions that initiate once glucose enters the cell. This correlates glycogen to the metabolic status of the organism. The journey of glucose towards glycogen is complex, and involves intracellular phosphorylation to glucose-6-phosphate, subsequent isomerisation to glucose-1-phosphate, then the formation of uridine 5′-diphosphate, which is then the monomeric unit used for glycogen synthesis.[8] The synthesis starts from a protein dimer, glycogenin, which autoglycosylates the initial short glucose chains, to which glycogen synthase polymerises further linear segments with α-1,4 linkages, and glycogen branching enzyme introduces α-1,6 branches.[6] The average chain length is composed of 10–14 glucose units.[9] Glycogen is then degraded in times of metabolic need by multiple enzymes, both in the cytosol (by glycogen phosphorylase and glycogen debranching enzyme) and in lysosomes (by lysosomal acid α-glucosidase).[8] The structure is therefore continuously fluctuating depending on glucose concentration.[10] A complete overview of glycogen metabolism can be found elsewhere.[8]

Glycogen properties

Glycogen can be isolated from multiple sources, including most mammalian organs,[11] oysters and mussels,[12] and from the kernels of sweet corn (termed phytoglycogen),[13] amongst others. In recent times, glycogen can be readily purchased commercially on the gram-to-tonne scale. The structural features of glycogen vary between these sources, including size, spanning from about 20 nm for bovine liver glycogen up to 80 nm for phytoglycogen, and molecular weight, spanning 3.6×10^5 Da (bovine liver) to 1.8×10^7 Da (phytoglycogen).[6] These properties are generally quite consistent from the same commercial source. The particles have an exceptionally high-water content, where a drastic change in dimensions occurs when they are dried. For example, bovine liver glycogen has a "wet" diameter of about 20 nm, and when dried on mica, the dimension normal to the mica (the height) reduces to about 2 nm.[14] The nanoparticles exhibit poor solubility in organic solvents (e.g., limited solubility in dimethyl sulfoxide and N,N-dimethylformamide), but very soluble in most aqueous systems. Glycogen precipitates readily in alcohol solvents, where in ethanol/water mixtures (35% v/v ethanol) phytoglycogen undergoes an approximate 80% decrease in volume,[15] before aggregating at higher ethanol fractions. Due to its high molecular weight, glycogen can also be dialysed with ease to

purify, allowing for green purification strategies. When functionalising, the functionalisation can come from the glucosyl units themselves, on the hydroxyl groups[14] or through ring-opening oxidation procedures,[16] but also from the small amount of protein left over from biological processes.[17] Glycogen can be degraded to smaller particle sizes through mild acid hydrolysis,[18] and, on the other hand, glycogen chains can be extended through enzymatic chain elongation, though this commonly leads to hydrogel materials as particles form stronger interactions together.[19] The nanoparticles have high water retention due to the abundance of closely-packed hydroxyl groups,[13] and can be functionalised to stick to most surfaces,[20] to inhibit corrosion,[21] to exhibit anti-inflammatory properties,[22] and encapsulating hydrophobic phases and vitamins,[23,24] antidotes,[25] amongst so much more. Whilst other biomaterials have been actively pursued in the nanomedicine space, including linear cellulose and branched starch polysaccharides, these other biomaterials lack the combined properties that are inherent to glycogen in its native nanoparticle form. These properties stem from glycogen's randomly hyperbranched structure from a central core; glycogen has a significantly higher branching density than, for example, amylopectin (the branched component of starch).[9] Furthermore, glycogen is naturally inside of us, meaning that we possess all the enzymatic machinery to degrade the nanoparticles, and that the nano-bio interface and interactions should be more predictable than for other nanomaterials. Using glycogen nanoparticles as an alternative to synthetic nanoparticles and other biomaterials has been gaining significant traction in recent years, and for good reason.

Targeting cancer and specific tissues

Glycogen, like most nanomaterial systems, are capable of passively accumulating in tumour tissue via the enhanced permeability and retention (EPR) effect, amongst other mechanisms. Filippov, et al.,[26] studied oyster glycogen nanoparticles coupled with a gandolinium motif for imaging the biological fate in vivo after intravenous injection into healthy mice. It was found that the nanoparticles do not accumulate significantly in the reticuloendothelial system, where the particles were eliminated in the urine. More recently, Galisova, et al.,[27] took a similar particle system and studied the fate in a rat model of hepatocellular carcinoma (HUH7 human cancer cell line), and monitored the biodistribution and clearance. The labelled particle systems exhibited no signs of toxicity or pathological changes in parachymal organs after administration, and with no necroinflammatory changes, steatosis or fibrosis in the liver tissue. The authors observed by magnetic resonance (MR) imaging and fluorescence in vivo imaging the accumulation of the glycogen-based conjugates in the tumour tissue, higher than the control, where the MR signals increased towards the tumour centre with time (Fig. 2A). This work highlights the multimodal capabilities of glycogen conjugates for solid tumour imaging.

These concepts can also be leveraged for external control over termination of cancer cells via, as example, photodynamic therapy. Shirinichi, et al.,[28] have reported on indocyanine green
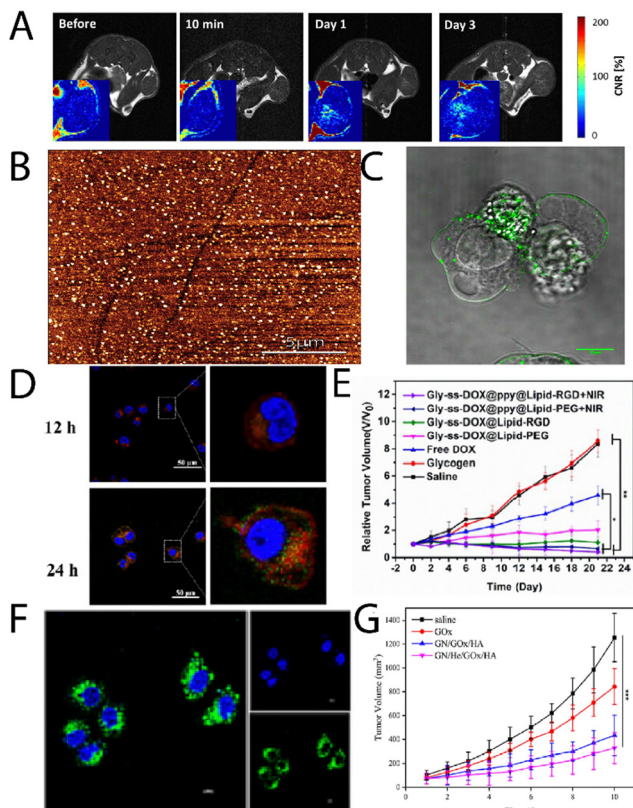
Fig. 2 (A) T_1-weighted images of rates injected with glycogen, with corresponding contrast-to-noise ratio maps (inserts) showing the accumulation of the probes in the tumour centers. Adapted from ref. 27. (B) AFM imaging of lactosylated glycogen nanoparticles that were used for (C) targeting prostate cancer PC3 cells. Adapted with permission from ref. 14. Copyright 2017 American Chemical Society. (D) CLSM images of Hep G2 cell uptake of Gly-ss-DOX-ppy@Lipid-PEG hybrids after 12 h and 24 h (nuclei, blue (DAPI); endosomes/lysosomes, green (lysotracker); particles, red), and (E) tumour volume of Hep G2 tumour bearing mice during treatment with different particle systems. Adapted with permission from ref. 31. Copyright 2020 American Chemical Society. (F) CLSM images of HeLa cells treated with GN/FITC-GOx/HA after 8 h, and (G) tumour weights with time for different treatment groups. Reprinted from ref. 32. Copyright 2023, with permission from Elsevier.

(ICG) coupled bovine liver glycogen nanoparticles for treatment of breast cancer cells. The hybrid nanoparticles dramatically increased the half-life of ICG from less than 4 h, to more than 100 h, and became highly cytotoxic only after administering near-infrared (NIR) light on MDA-MB-231 human breast cancer cells. These concepts of targeted external control over glycogen conjugates can be expanded upon on many fronts, particularly within the framework of 4D nanomaterials.

Aside from passive targeting, glycogen can readily be engineered to specifically target cancer tissue. Besford, *et al.*,[14] developed galactosylated bovine liver glycogen nanoparticles for targeting prostate cancer (PC3) cells. The particles were well dispersed (Fig. 2B) after copper(I)-catalysed click chemistry conjugation of a lactose-azide. The conjugates exhibited strong interaction with β-galactoside specific lectins *ex situ* (*e.g.*, peanut agglutinin), but importantly, *in vitro* with PC3 cells (Fig. 2C). A multivalent effect was observed with the clustering

of the cells after administering the conjugates. This was inferred to come from specific extracellular targeting of galectin-1, which is overexpressed on PC3 cell membranes. Importantly, this demonstrated direct cancer cell targeting from functional glycogen nanoparticles, whereas the native bovine liver glycogen nanoparticles did not exhibit such targeting. Han, *et al.*,[29] took the concept a step further for targeted drug delivery to liver cancer cells, using β-galactose modification *via* a Schiff-base reaction with an aminated β-galactose derivative. The drug, doxorubicin (DOX), was conjugated by the same strategy. The conjugates drastically increased the circulation half-life of the DOX and led to a reduction in the relative tumour volume with time after administering. Whilst the results were promising, it should be separately commented that the Schiff-base strategy is typically unstable under aqueous conditions – a simple reductive amination eliminates this stability risk.[30]

Zhou, *et al.*,[31] developed glycogen/drug/polypyrrole hybrids coated with a phospholipid layer and RGD peptide for targeting liver cancer cells. Drugs were conjugated *via* disulphide coupling, which exhibited glutathione-triggered cleavage, where the polypyrrole allowed for near infrared (NIR)-absorption and therefore a phototherapeutic treatment option (external control). The conjugates were found to uptake in Hep G2 cells, with lysosomal escape after 6 h, and very little overlap of the lysosome and particle signals after 24 h incubation (Fig. 2D; lysotracker, green; DOX, red). Furthermore, the authors observed significant accumulation in liver tumours, with reductions in tumour volumes in the presence of NIR light (Fig. 2E). A similar strategy was recently explored by Li, *et al.*,[33] who developed glycogen modified with lactobionic acid (terminal β-galactose) amongst other motifs, for targeted delivery of resveratrol to the liver in high-fat diet-induced non-alcoholic fatty liver disease. It was found that the conjugates could successfully reduce lipid deposition and oxidative stress, and relieve inflammation symptoms in mice.

Other work has explored the coupling of functional enzymes to glycogen. Qiu, *et al.*,[32] recently reported on a glycogen/hemin/glucose oxidase (GOx) hybrid composites, decorated with hyaluronic acid (HA). These were used to co-deliver hemin and GOx to tumour cells, where the GOx oxidises intracellular glucose (also supplied from degraded glycogen), and the hemin catalyses the Fenton reaction, leading to the production of reactive oxygen species (ROS) and ultimately cell death. The authors were able to achieve internalisation of the GOx (Fig. 2F) and a significant difference in tumour volume for the 4-component system in comparison to the control system (Fig. 2G). A similar strategy was reported by Yang, *et al.*,[34] who leveraged hyaluronan-cyclodextrin for targeting to CD44 cells, whilst allowing for host–guest interactions with ferrocene. The authors observed tumour targeting and tumour suppression *in vivo* in HeLa tumour bearing mice. A separate enzymatic system has been reported by Zhang, *et al.*,[35] that involved functionalising glycogen with phenylboronic acid motifs after sodium meta periodate-mediated oxidation, which then allowed for coupling to the enzyme carbonic anhydrase. Such functional hybrids may have interesting applications on a variety of fronts.

Overall, targeting motifs can be conjugated covalently, as discussed for β-galactosides, but can also be electrostatically adsorbed onto cationic glycogen, or tethered by host–guest chemistry. The conjugation strategies are therefore robust, however the end biodegradability should always be checked of the functionalised systems,[14] when biodegradability is important for the purpose.

Nucleic acid and peptide delivery

Towards other technologies, the use of nucleic acids, such as small interfering RNA (siRNA) and double-stranded RNA, have been increasing in the field. Various glycogen constructs have been designed to interact and ''hold'' nucleic acids to protect the structures and facilitate delivery both to cells and 3D tissue scaffolds. The most common strategy is to bind nucleic acids electrostatically to positively charged glycogen. Cationic glycogens can be generated by a variety of methods, including esterification reactions with triphenylphosphine via carboiimide coupling (Fig. 3A), by reacting glycogen with alkylamino alkyl chloride derivatives under basic conditions (Fig. 3B), oxidation and reductive amination with ethylenediamine (EDA) (Fig. 3C), and epoxide ring-opening coupling with glycidyltrimethylammonium chloride (Fig. 3D). The ζ-potential of these derivatives generally spans about +20 to +40 mV. Glycogen-nucleic acid hybrids are formed by mixing negatively charged nucleic acids with cationic glycogen at specific ratios to form glycoplexes.

Chen, et al.,[36] have recently reported triphenylphosphine functionalised glycogen for complexing surviving siRNA with delivery to HeLa cells, where it was observed the hybrids were uptaken by tumour cells, escaped from lysosomes, resulting in good gene transfection efficiencies. Engelberth, et al.,[38] found that enzymatically synthesised glycogen (cESG)-siRNA hybrids exhibited specific uptake by ES-2 ovarian clear cell carcinoma cells depending on the amount of siRNA per glycoplex (Fig. 4A), and allowed for sustained siRNA delivery for up to 6 days with less toxicity than the lipofectamine standard. Racaniello, et al.,[37] developed mussel glycogen-Hs Cell Death siRNA hybrids for inducing cell death, where cells transfected with lipofectamine and the cationic glycogen-siRNA hybrid (DEAE) induced cell death in HK2 cells (green regions Fig. 4B). Alkie, et al.,[39] looked to increase innate antiviral immune responses in rainbow trout RTgutGC cells through delivery of high

Fig. 4 (A) Uptake of fluorescently labelled siRNA/cESG complexes by ES-2 ovarian clear cell carcinoma cells, bright field with overlay (left) and fluorescence (right), of the cells after incubation for 72 h. Reprinted with permission from ref. 38. Copyright 2015 American Chemical Society. (B) Fluorescence intensity per cell of the glycogen/dsRNA complexes, and the relative mRNA expression profiles for IFN1 measured after 3 h. Reprinted from ref. 37. Copyright 2021, with permission from Elsevier. (C) Uptake of Poly(I : C)HMW and Nano-HMW into RTgutGC cells after 3 h at 20 °C, and (D) relative mRNA expression profiles for IFN1 measured after 3 h, adapted from ref. 39. (E) Scanning electron microscopy image of DMAPA-Glyp/siRNA complexes, and (F) suppression on the protein expression of the NF-κB p65 gene as evaluated from Western blot analysis. Adapted from ref. 43.
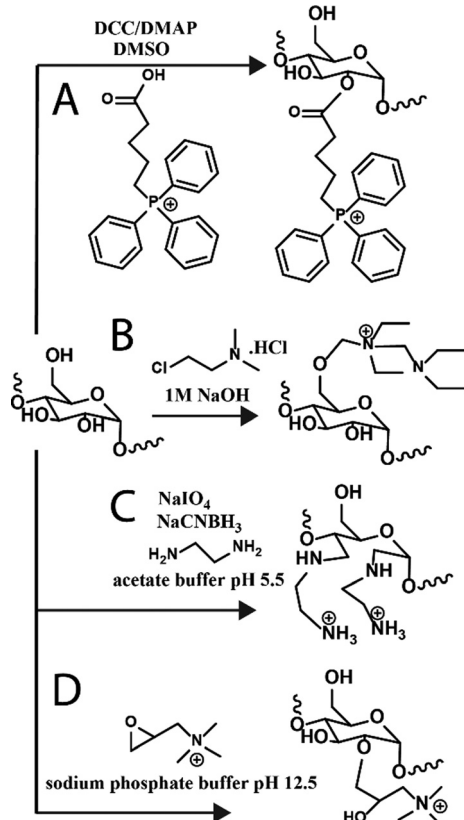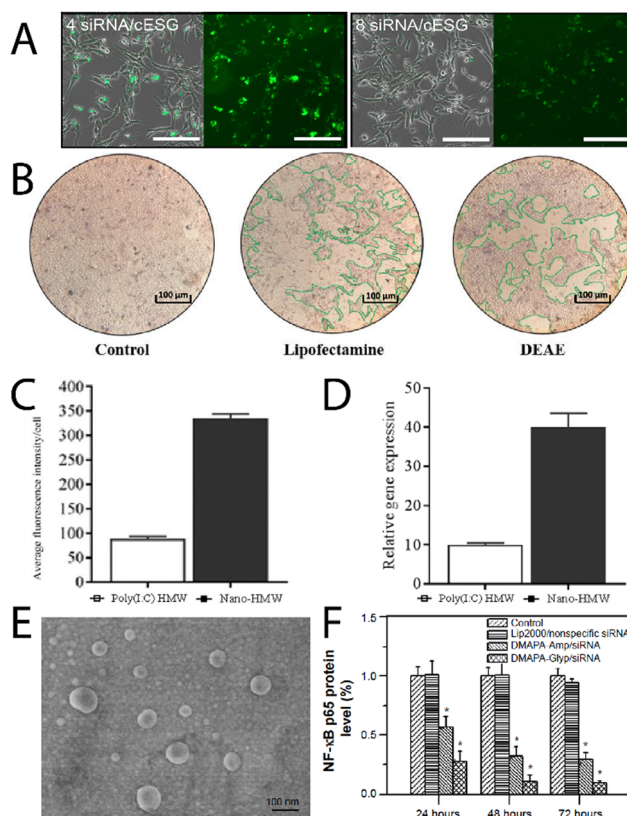

Fig. 3 Reaction schematics for generating cationic glycogens. Further details for reactions (A)–(D) can be found in ref. 36, 37, 30 and 38, respectively.

molecular weight polyinosinic : polycytidylic acid (poly(I : C)) (a synthetic analogue of double stranded RNA) conjugated to phytoglycogen nanoparticles (Nano-HMW), which exhibited increased cell targeting and significantly upregulated type 1 interferons (IFNs) (Fig. 4C and D, respectively). Lewis, et al.,[40] investigated the use of cationic phytoglycogen for delivering poly(I : C) to ovarian cancer (OVCAR-3) cells. It was found that there was clear uptake of the hybrid clusters and that the nanoparticles without cargo exhibited no cytotoxicity to the OVCAR-3 cells, but with the poly(I : C) cargo the clusters became highly cytotoxic with activation of capases-3/-7. Zhang, et al.,[41] used cationic glycogen reacted with an oxidised yeast β-glucan, specifically recognised by dectin-1 on macrophages, which was electrostatically complexed with CpG oligodeoxynucleotides. This allowed for macrophage targeted immunostimulation, after lysosomal degradation of the glycogen component by α-glucosidase.[42]

Elsewhere, Liu, et al.,[43] recently developed oyster glycogen-siRNA hybrids for inhibition of nuclear transcription factor-kappa B (NF-κB) in human retinal pigment epithelial (hRPE) cells in diabetic retinopathy. The NF-κB is thought to play an important role in the angiogenesis of diabetic retinopathy due to expression of various factors that lead to retinal neovascularisation. The clusters (DMAPA-Glyp/siRNA) were disperse (Fig. 4E), and exhibited cell uptake of between about 70 to 95% efficiency, and successfully suppressed the protein expression of the NF-κB p65 gene, and even more so than another polysaccharide hybrid (amylopectin; DMAPA-Amp/siRNA) (Fig. 4F), likely due to the better incorporation of siRNA amongst the oyster glycogen chains. Further on diabetes treatments, Lan, et al.,[44] developed cationic glycogen-siRNA hybrids for treating diabetic wounds in rats. The system demonstrated knockdown of MMP-9 of skin wound tissues, with ultimate enhanced wound healing. As an aside, but in a similar vein, Jenik, et al.,[45] used inosine monophosphate-conjugated phytoglycogen nanoparticles for enhancing cell proliferation of a bovine intestinal myofibroblast cell line.

The nucleic acid works highlight that glycogen hybrids can not only protect and deliver nucleic acids to target cells, but that the hybrids can successful rupture the endosomes and allow for the cystolic release of the functional cargo, as shown via super resolution imaging of bovine liver glycogen-siRNA clusters by Wojnilowic, et al.[46] Similarly, Bhangu, et al.,[47] have recently shown that cationic phytoglycogen nanoparticles can carry an oligonucleotide probe, prevent its degradation, and facilitate its intracellular trafficking from early to late endosomes within 2 h of incubation, and ultimately endosomal escape and cystolic release of the oligonucleotide with longer times. These cationic glycogen nanoparticle systems can therefore be carefully designed for effective intracellular and sustained delivery of nucleic acids, where the conjugation strategies to make the glycogen carrier are most often simple.

Moving towards more complex 3D tissues and systems that encounter the natural immune system in blood, Wojnilowicz, et al.,[30] developed cationic bovine liver glycogen-siRNA constructs for gene silencing in both multicellular tumour spheroids of PC3 human prostate cancer cells, and HEK-293T human kidney epithelial cells. The system was successfully able to penetrate into the complex 3D spheroids and mediate gene silencing of luciferase in 293T cells, and survivin in PC3 cells, which was comparable to the commercial transfection agent lipofectamine RNAiMax. When the constructs were injected into healthy mice, it was found they had a circulation lifetime of about 8 h, with preferential accumulation in the liver, and no accumulation in the kidney, lung, spleen, heart, or brain. Later, Wojnilowicz, et al.,[48] investigated the influence of the protein corona on cationic bovine liver glycogen-siRNA hybrid gene silencing with ex vivo human immune cells. The authors
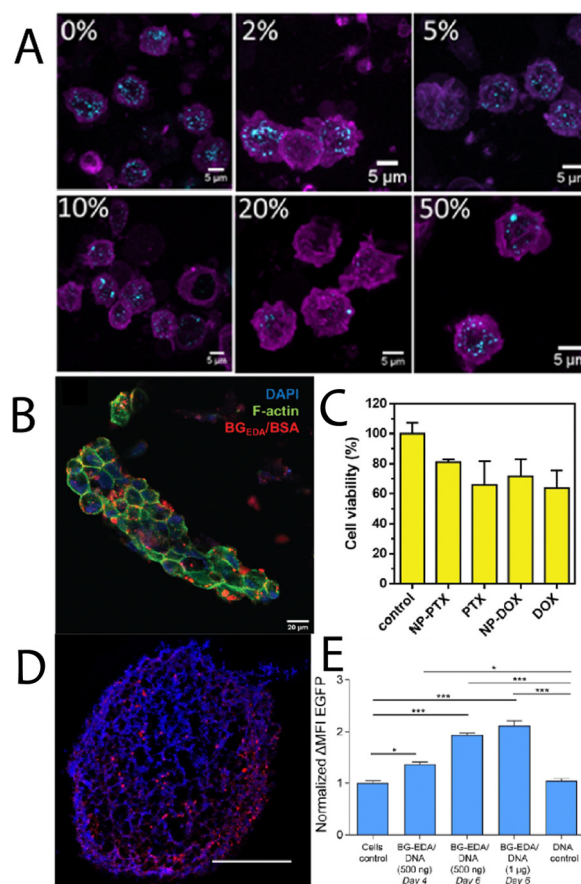

Fig. 5 (A) Maximum intensity CLSM projections showing internalisation of cationic glycogen-siRNA complexes by monocytes treated with different concentrations of human serum (complexes depicted in cyan, cell membranes in magenta). Adapted with permission from ref. 48. Copyright Elsevier 2022. (B) CLSM image of a collagen scaffold co-cultured with NIH-3T3 cells, BT-474 cells, and Raw 264.7 cells, stained for F-actin (phalloidin; green) and nucleus (DAPI; blue) after incubation with cationic glycogen-albumin constructs (red) for 24 h, and (C) cytotoxicity of the complexes loaded with PTX and DOX in the same cells grown in a 3D perfusion reactor after 24 h, compared to the free drugs. Adapted from ref. 49. (D) CLSM image showing the distribution of cationic bovine liver glycogen (stained with Alexa-Fluor 647; red) in the center of a sensory neurosphere (nucleus stained with Hoeschst; blue), and (E) EGFP gene expression after transfection with the particle-plasmid DNA hybrids. Adapted with permission from ref. 50. Copyright 2020 American Chemical Society.

observed that the interaction between primary monocytes and the glycogen-siRNA hybrids was minimised in the presence of increasing concentration of serum proteins (Fig. 4A), with the adsorbed components particularly rich in serum albumin, haptoglobin, alpha-1-antitrypsin, and apolipoprotein A-II, amongst others. Radziwon, et al.,[49] recently reported on cationic bovine liver glycogen-albumin hybrid constructs as pH-responsive scaffolds that can undergo endosomal escape in tumour, stromal and immune cells, whilst carrying therapeutic agents. It was observed that the hybrid nanomaterials could successfully penetrate tumour-mimicking tissues in 3D
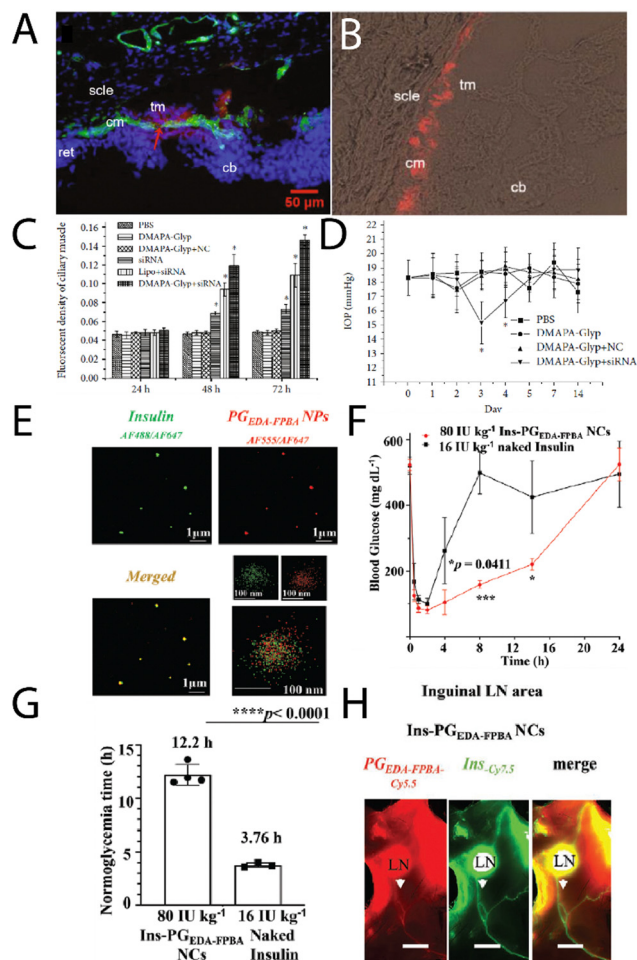

Fig. 6 (A) A merged fluorescence microscopy images of cationic glycogen-siRNA conjugates (DMAPA-Gly/Cy3-siRNA) after intracameral injection into the rat ciliary muscle (nuclei, blue; ciliary muscle, green; conjugates, red; cm-ciliary muscle; cb-ciliary body; ret-retina; scle-sclera; tm-trabecular meshworks), and (B) fluorescence microscopy image of the conjugates in the ciliary muscle after 72 h, with (C) the fluorescence of the muscle as a function of time, and (D) changes in the IOP with time after transfection. Adapted from ref. 51. (E) multi-colour STORM images of insulin (green) – glycogen (red) conjugates, (F) blood glucose levels in Akita type 1 diabetic mice after treatment with naked insulin, insulin-glycogen conjugates (Ins-PG$_{EDA-FPB}$ NCs), and the functional glycogen (Ins-PG$_{EDA-FPB}$ NPs), along with (G) normalglycemic times for the treatments, and (H) NIR images of the insulin-glycogen conjugates in inguinal LNs 24 h after subcutaneous injection (Akita mice – scale bar 3 mm). Reprinted in part with permission from ref. 52. Copyright 2023 John Wiley and Sons.

(Fig. 5B) and induce cell death with either DOX or paclitaxel (PTX) (Fig. 5C) as therapeutic cargo. The conjugate with a model protein (albumin) establishes an intriguing basis for further glycogen-protein conjugates for protein delivery. Cuba-Wojnilowicz, et al.,[50] have shown that cationic bovine liver glycogen nanoparticles could complex plasmid DNA to form structures about 180 nm in diameter that could penetrate human embryonic stem cell-derived 3D cell cultures of sensory neurons (called sensory neurospheres) (Fig. 5D). The hybrid system could successfully deliver functional plasmid DNA leading to gene expression in neurons up to 6 days post-transfection (Fig. 5E).

Zeng, et al.,[51] investigated cationic oyster glycogen derivatives with complexed siRNA for IκBα gene silencing in the ciliary muscle of rat eyes. The authors explored the role of the IκB/NF-κB signaling pathway in the uveoscleral outflow pathway. It was found that a large amount of the complexes were found in the ciliary muscle after intracameral injection (Fig. 6A and B), where the complexes remained for up to 72 h, likely due to transport via the unconventional outflow pathway. This provided the complexes more opportunity to transfect in the ciliary muscle (Fig. 6C), resulting in a reduction of the intraocular pressure (IOP) after 72 h (Fig. 6D), potentially a treatment option for glaucoma.

An exciting new strategy for administering glycogen nanoparticles has recently been reported by Xu, et al.,[52] who developed cationic phytoglycogen with functional phenylboronic acid (PBA) units. This allowed for electrostatic complexation with a negatively charged peptide (insulin) (Fig. 6E), where in the presence of high glucose concentration the PBAs formed phenyl boronic esters with glucose leading to a negative charge. This switch in charge meant the insulin decomplexed and was released into solution, used as a treatment in diabetic mice. After a single subcutaneous injection of the complexes, a rapid and sustained response to a glucose challenge in diabetic mice was observed (Fig. 6F), with optimal blood glucose levels achieved for up to 13 h (Fig. 6G), enabled from the pharmacokinetics of the complexes. Interestingly the glycogen-insulin complexes were detected in the inguinal lymph nodes and associated lymphatic vessels 24 h post-subcutaneous injection (Fig. 6H), indicating the transport of the complexes by the lymphatic system before eventually reaching systemic circulation. The complexes were still found in the blood several days after subcutaneous injection. This strategy of subcutaneous injections of glycogen nanoparticles may likely prove to be a viable route of administration for treating other conditions.

The development of other glycogen-peptide conjugates for delivery is thus far scarce in the literature, but certainly an exciting front for further investigations.

Conclusions and outlook

The recent research works in nanomedicine that utilise glycogen as a key carrier system serves to emphasise the numerous opportunities in applications of these unique nanoparticles.

These studies highlight aspects of glycogen's inherent biological properties, which gives significant advantages to other bottom-up synthetic nanoparticles. Especially given that glycogen is a reasonably low-cost off-the-shelf product, which is ultimately biodegradable by glucosidase enzymes in most cells, yielding sugar and a minor amount of protein. This is a strong benefit that cannot easily be matched by synthetic alternatives. The benefit of a biocompatible and biodegradable, off-the-shelf nanoparticle can also not easily be matched by other biomaterials.

Moving forward, it will be useful for the field to better understand source-dependent effects of glycogen nanoparticles – it is known that glycogen nanoparticles differ in the protein content depending on the source.[17] How this affects bio-nano interactions, particularly in-blood (inflammation, immune cell association, etc.) remains largely unknown. Likewise, it is crucial to determine how extra grafted motifs for functionality, targeting, or as the therapeutic cargo, affects in vivo pharmacokinetics, cell internalisation, and biodegradability.[17,30,53] Additionally, exploring the evolution of chain packing density, end-groups, and branching with particle size[2,54–56] may allow for new understanding on how to couple multimodal functionalities into the nanoparticles, particularly on ''burying'' therapeutics amongst the internal polymer chains.

The focus herein has only been on dispersed nanoparticle-based glycogen systems, particularly on how these nanoparticles can be nano-engineered for targeting tissues, delivering drugs, nucleic acids, and peptides. Focus was not given to the area of glycogen as a key component in macroscopic hydrogel/adhesive/tissue regeneration technologies, which is a separate but equally exciting area. However, it is at least clear that glycogen nanoparticles hold very real potential as viable, renewable, biocompatible and biodegradable components in nanomedicine going forward, where these sugary nanoparticles can be leveraged back into biology to do some good.

Conflicts of interest

There are no conflicts to declare.

Acknowledgements

References

1 Q. H. Liu, J. W. Tang, P. B. Wen, M. M. Wang, X. Zhang and L. Wang, *Front. Mol. Biosci.*, 2021, **8**, 673315.

2 Q. A. Besford, X. Y. Zeng, J. M. Ye and A. Gray-Weale, *Glycoconjugate J.*, 2016, **33**, 41–51.

3 F. G. Young, *Br. Med. J.*, 1957, **5033**, 1432–1437.

4 W. B. Hannah, T. G. J. Derks, M. L. Drumm, S. C. Grunert, P. S. Kishnani and J. Vissing, *Nat. Rev. Dis. Primers*, 2023, **9**, 46.

5 J. Dolai, K. Mandal and N. R. Jana, *ACS Appl. Nano Mater.*, 2021, **4**, 6471–6496.

6 Q. A. Besford, F. Cavalieri and F. Caruso, *Adv. Mater.*, 2020, **32**, e1904625.

7 M. Gericke, A. J. R. Amaral, T. Budtova, P. De Wever, T. Groth, T. Heinze, H. Hofte, A. Huber, O. Ikkala, J. Kapusniak, R. Kargl, J. F. Mano, M. Masson, P. Matricardi, B. Medronho, M. Norgren, T. Nypelo, L. Nystrom, A. Roig, M. Sauer, H. A. Schols, J. van der Linden, T. M. Wrodnigg, C. Xu, G. E. Yakubov, K. Stana Kleinschek and P. Fardim, *Carbohydr. Polym.*, 2024, **326**, 121633.

8 M. M. Adeva-Andany, M. Gonzalez-Lucan, C. Donapetry-Garcia, C. Fernandez-Fernandez and E. Ameneiros-Rodriguez, *BBA Clin.*, 2016, **5**, 85–100.

9 D. J. Manners, *Carbohydr. Polym.*, 1991, **16**, 37–82.

10 Z. Hu, B. Deng, X. Tan, H. Gan, C. Li, S. S. Nada, M. A. Sullivan, J. Li, X. Jiang, E. Li and R. G. Gilbert, *Carbohydr. Polym.*, 2018, **185**, 145–152.

11 Q. A. Besford, M. A. Sullivan, L. Zheng, R. G. Gilbert, D. Stapleton and A. Gray-Weale, *Int. J. Biol. Macromol.*, 2012, **51**, 887–891.

12 J.-H. Ryu, J. Drain, J. H. Kim, S. McGee, A. Gray-Weale, L. Waddington, G. J. Parker, M. Hargreaves, S.-H. Yoo and D. Stapleton, *Int. J. Biol. Macromol.*, 2009, **45**, 478–482.

13 V. Adibnia, Y. Ma, I. Halimi, G. C. Walker, X. Banquy and E. Kumacheva, *ACS Nano*, 2021, **15**, 8953–8964.

14 Q. A. Besford, M. Wojnilowicz, T. Suma, N. Bertleff-Zieschang, F. Caruso and F. Cavalieri, *ACS Appl. Mater. Interfaces*, 2017, **9**, 16869–16879.

15 T. Kamarainen, K. Kadota, J. Y. Tse, H. Uchiyama, T. Oguchi, H. Arima-Osonoi and Y. Tozuka, *Biomacromolecules*, 2023, **24**, 225–237.

16 M. Bertoldo, G. Zampano, L. Suffner, E. Liberati and F. Ciardelli, *Polym. Chem.*, 2013, **4**, 653–661.

17 Q. A. Besford, A. C. G. Weiss, J. Schubert, T. M. Ryan, M. F. Maitz, P. P. Tomanin, M. Savioli, C. Werner, A. Fery, F. Caruso and F. Cavalieri, *ACS Appl. Mater. Interfaces*, 2020, **12**, 38976–38988.

18 B. Pan, N. Zhao, Q. Xie, Y. Li, B. R. Hamaker and M. Miao, *NPJ Sci. Food*, 2023, **7**, 27.

19 H. Izawa, M. Nawaji, Y. Kaneko and J. Kadokawa, *Macromol. Biosci.*, 2009, **9**, 1098–1104.

20 P. Pacchin Tomanin, J. Zhou, A. Amodio, R. Cimino, A. Glab, F. Cavalieri and F. Caruso, *J. Mater. Chem. B*, 2020, **8**, 4851–4858.

21 M. Pais, S. D. George and P. Rao, *Int. J. Biol. Macromol.*, 2021, **182**, 2117–2129.

22 Y. Xu, B.-W. Zhu, X. Li, Y.-F. Li, X.-M. Ye and J. N. Hu, *Biomaterials*, 2022, **280**, 121077.

23 R. Cimino, S. K. Bhangu, A. Baral, M. Ashokkumar and F. Cavalieri, *Molecules*, 2021, **26**, 5157.

24 X. Mao, L. Long, J. Shen, K. Lin, L. Yin, J. Yi, L. M. Zhang, D. Y. B. Deng and L. Yang, *Food Funct.*, 2021, **12**, 8522–8534.

25 H. Zhukouskaya, P. M. Blanco, Z. Cernochova, L. Ctverackova, R. Stano, E. Pavlova, M. Vetrik, P. Cernoch, M. Filipova, M. Slouf, M. Stepanek, M. Hruby, P. Kosovan and J. Panek, *Biomacromolecules*, 2022, **23**, 3371–3382.

26 S. K. Filippov, O. Sedlacek, A. Bogomolova, M. Vetrik, D. Jirak, J. Kovar, J. Kucka, S. Bals, S. Turner, P. Stepanek and M. Hruby, *Macromol. Biosci.*, 2012, **12**, 1731–1738.

27 A. Galisova, M. Jiratova, M. Rabyk, E. Sticova, M. Hajek, M. Hruby and D. Jirak, *Sci. Rep.*, 2020, **10**, 10411.

28 F. Shirinichi, C. Karkera, T. Ibrahim, H. Khan, T. Clemons, A. G. Senejani and H. Sun, *Macromol. Chem. Phys.*, 2023, **224**, 2300327.

29 Y. Han, B. Hu, M. Wang, Y. Yang, L. Zhang, J. Zhou and J. Chen, *Appl. Mater. Today*, 2020, **18**, 100521.

30 M. Wojnilowicz, Q. A. Besford, Y. L. Wu, X. J. Loh, J. A. Braunger, A. Glab, C. Cortez-Jugo, F. Caruso and F. Cavalieri, *Biomaterials*, 2018, **176**, 34–49.

31 J. Zhou, Y. Han, Y. Yang, L. Zhang, H. Wang, Y. Shen, J. Lai and J. Chen, *ACS Appl. Mater. Interfaces*, 2020, **12**, 23311–23322.

32 L. Qiu, J. Wang, M. Conceicao, S. Liu, M. Yang, W. Chen, M. Long, X. Cheng, M. J. A. Wood and J. Chen, *Int. J. Biol. Macromol.*, 2023, **239**, 124363.

33 X. Li, X. X. Chen, Y. Xu, X. B. Xu, W. F. Wu, Q. Zhao and J. N. Hu, *Biomacromolecules*, 2022, **23**, 409–423.

34 F. Yang, W. Fang, M. Yang, W. Chen, J. Xu, J. Wang, W. Li, B. Zhao, L. Qiu and J. Chen, *Int. J. Biol. Macromol.*, 2022, **217**, 878–889.

35 D. Zhang, Z. Wang, J. Gu, Y. Zhang and J. Chen, *J. Polym. Sci.*, 2024, **62**, 806–814.

36 Z. Chen, M. Su, J. Xu, J. Li, G. Wangcao and L. Qiu, *J. Drug Delivery Sci. Technol.*, 2024, **92**, 105371.

37 G. F. Racaniello, V. Laquintana, J. Vergnaud, A. Lopedota, A. Cutrignelli, A. Lopalco, F. Leonetti, M. Franco, M. Fiume, P. Pontrelli, L. Gesualdo, E. Fattal and N. Denora, *Int. J. Pharm.*, 2021, **608**, 121128.

38 S. A. Engelberth, N. Hempel and M. Bergkvist, *Bioconjugate Chem.*, 2015, **26**, 1766–1774.

39 T. N. Alkie, J. de Jong, K. Jenik, K. M. Klinger and S. J. DeWitte-Orr, *Sci. Rep.*, 2019, **9**, 13619.

40 A. Lewis, A. Tran, N. L. Aldor, N. A. Jadaa, T. Feng, E. Moore, S. J. DeWitte-Orr and S. J. Poynter, *J. Nanopart. Res.*, 2023, **25**, 104.

41 H. Zhang, K. Ma, H. Liu, S. Wang, Z. Wang, J. Zhang and J. Chen, *ACS Appl. Nano Mater.*, 2023, **6**, 22480–22487.

42 H. Zhang, L. Lai, Z. Wang, J. Zhang, J. Zhou, Y. Nie and J. Chen, *Int. J. Biol. Macromol.*, 2024, **257**, 128536.

43 Z. Liu, H. Gong, R. Zeng, X. Liang, L. M. Zhang, L. Yang and Y. Lan, *Int. J. Nanomed.*, 2015, **10**, 2735–2749.

44 B. Lan, J. Wu, N. Li, C. Pan, L. Yan, C. Yang, L. Zhang, L. Yang and M. Ren, *Int. J. Biol. Macromol.*, 2020, **154**, 855–865.

45 K. Jenik, T. N. Alkie, E. Moore, J. D. Dejong, L. E. J. Lee and S. J. DeWitte-Orr, *In Vitro Cell. Dev. Biol.: Anim.*, 2021, **57**, 86–94.

46 M. Wojnilowicz, A. Glab, A. Bertucci, F. Caruso and F. Cavalieri, *ACS Nano*, 2019, **13**, 187–202.

47 S. K. Bhangu, L. Mummolo, S. Fernandes, A. Amodio, A. Radziwon, B. Dyett, M. Savioli, N. Mantri, C. Cortez-Jugo, F. Caruso and F. Cavalieri, *Adv. Funct. Mater.*, 2024, 2311240.

48 M. Wojnilowicz, P. Laznickova, Y. Ju, C. S. Ang, F. Tidu, K. Bendickova, G. Forte, M. Plebanski, F. Caruso, F. Cavalieri and J. Fric, *Biomater. Adv.*, 2022, **140**, 213083.

49 A. Radziwon, S. K. Bhangu, S. Fernandes, C. Cortez-Jugo, R. De Rose, B. Dyett, M. Wojnilowicz, P. Laznickova, J. Fric, G. Forte, F. Caruso and F. Cavalieri, *Nanoscale*, 2022, **14**, 3452–3466.

50 E. Czuba-Wojnilowicz, S. Miellet, A. Glab, S. Viventi, F. Cavalieri, C. Cortez-Jugo, M. Dottori and F. Caruso, *Biomacromolecules*, 2020, **21**, 3186–3196.

51 R. Zeng, J. Li, H. Gong, J. Luo, Z. Li, Z. Ou, S. Zhang, L. Yang and Y. Lan, *Biomed. Res. Int.*, 2020, **2020**, 8206849.

52 R. Xu, S. K. Bhangu, K. C. Sourris, D. Vanni, M. A. Sani, J. A. Karas, K. Alt, B. Niego, A. Ale, Q. A. Besford, B. Dyett, J. Patrick, I. Carmichael, J. E. Shaw, F. Caruso, M. E. Cooper, C. E. Hagemeyer and F. Cavalieri, *Adv. Mater.*, 2023, **35**, e2210392.

53 M. Jiratova, A. Pospisilova, M. Rabyk, M. Parizek, J. Kovar, A. Galisova, M. Hruby and D. Jirak, *Drug Delivery Transl. Res.*, 2018, **8**, 73–82.

54 P. Zhang, S. S. Nada, X. Tan, B. Deng, M. A. Sullivan and R. G. Gilbert, *Int. J. Biol. Macromol.*, 2018, **116**, 264–271.

55 D. Kim and J. Duhamel, *Carbohydr. Polym.*, 2023, **299**, 120205.

56 Y. Rousset, O. Ebenhoh and A. Raguin, *PLoS Comput. Biol.*, 2023, **19**, e1010694.